Journal of
Applied Remote Sensing

RemoteSensing.SPIEDigitalLibrary.org

Spatial–temporal variations of vegetation and drought severity across Tharparkar, Pakistan, using remote sensing-derived indices

Sami Ullah Shah
Javed Iqbal

SPIE.

Sami Ullah Shah, Javed Iqbal, "Spatial–temporal variations of vegetation and drought severity across Tharparkar, Pakistan, using remote sensing-derived indices," *J. Appl. Remote Sens.* **10**(3), 036005 (2016), doi: 10.1117/1.JRS.10.036005.

Spatial–temporal variations of vegetation and drought severity across Tharparkar, Pakistan, using remote sensing-derived indices

Sami Ullah Shah and Javed Iqbal*
National University of Sciences and Technology, Institute of Geographical Information Systems, School of Civil and Environmental Engineering, Islamabad, Pakistan

Abstract. Tharparkar is an arid region in the southeastern province of Sindh, Pakistan, and experienced drought as a regular phenomenon in the past. The complex nature of drought and sparsely located network of met stations handicapped reliable spatial and temporal analysis of drought severity across Tharparkar. Freely available tropical rainfall measuring mission rainfall satellite data and moderate-resolution imaging spectroradiometer normalized difference vegetation index (NDVI) satellite data fulfilled this gap and were used to generate drought indices. Commonly used NDVI and NDVI anomalies pose problems when compared with standardized meteorological drought indices such as standardized precipitation index (SPI) and standardized precipitation and evapotranspiration index (SPEI) for drought characterization. This study compared standardized vegetation index (SVI) with traditionally used, i.e., SPI and SPEI, for modeling drought severity in the arid and fragile agro-ecosystem of Tharparkar. SVI significantly correlated with standardized meteorological drought indices (SPI and SPEI) and revealed vegetation dynamics under rainfall and temperature variations. Weighted overlay analysis in geographical information systems depicted an accurate onset of the 2014 drought. This study provides useful information for drought characterization that can be used for drought monitoring and early warning systems in data scarce, arid, and semiarid regions. © *2016 Society of Photo-Optical Instrumentation Engineers (SPIE)* [DOI: 10.1117/1.JRS.10.036005]

Keywords: remote sensing-derived indices; drought; Tharparkar; Pakistan.

Paper 16192 received Apr. 6, 2016; accepted for publication Jun. 17, 2016; published online Jul. 12, 2016.

1 Introduction

Drought is a natural calamity that develops after abnormally low or no rainfall for some time period.[1] Droughts occur at a slow rate but are one of the natural disasters that inflict heavy human and economic losses. Droughts are difficult to quantify as they occur at a slow pace, slowly creeping in and hence pose problems with quantification of onset, end, and spatial extent.[2] Useable water sources related to drought are affected at different time scales. Reservoir storage, ground water, soil moisture, and stream flow are some of the useable resources where deficits occur due to drought at certain time periods. Therefore, the time scale at which water deficit occurs in a particular water source forms an important characteristic of drought and functionally separates different types of droughts.[1] Four types of droughts have been identified in the literature, i.e., meteorological, agricultural, hydrological, and socioeconomical.[3] These drought types differ from one another in duration, intensity, and spatial coverage depending upon time period for which the drought prevails.[4] Deficiency in precipitation causes meteorological drought, while lack of volume of water supply in channels and reservoir storage leads to hydrological drought.[5] Instead, agricultural drought is categorized by inadequate soil water level in the root zone due to excessive water losses caused by evapotranspiration[6] and prolonged shortage of water.[7] Socioeconomic drought is related with the supply and demand phase of

*Address all correspondence to: Javed Iqbal, E-mail: javed@igis.nust.edu.pk

economic goods.[8] The meteorological and agricultural droughts are quantified at temporal scales of 1 to 6 months, whereas hydrological droughts are quantified at temporal scales of 6 to 24 months.[4]

Numerous objective indices have been developed worldwide for quantitation and monitoring of droughts using various data, primarily meteorological and vegetation data. However, these data are not generally available for far flung arid regions in developing countries. Nonavailability of reliable data constrains the institutional ability of governments to quantify spatial and temporal extents of drought severity and hence leaves them with insufficient knowledge in regard to the management of drought events. Remote sensing of meteorological and vegetation data can fill this gap with remotely sensed meteorological and vegetation data at a variety of spatial and temporal scales.[9] Naumann et al.[10] used tropical rainfall measuring mission (TRMM) monthly rainfall data for monitoring drought over Africa. Du et al.[11] integrated TRMM rainfall data with moderate-resolution imaging spectroradiometer (MODIS) vegetation data for drought monitoring over Shandong, China. Rhee et al.[12] used TRMM rainfall data to monitor drought and suggested that in case of sparse *in situ* data, remote sensing data can be used alone or in combination with *in situ* data. Yaduvanshi et al.[13]used TRMM rainfall and MODIS normalized difference vegetation index (NDVI) data to develop drought indices for drought monitoring over tropical regions in India. Li et al.[14] used remote sensing-derived vegetation index to assess agricultural drought in semiarid regions of China. Dutta et al.[15] 2015 used remote sensing-derived index to assess agricultural drought across Rajasthan, India.

Numerous objective indices have been developed worldwide for quantitation and monitoring of droughts using various parameters. However, versatility in definition of drought made it difficult to develop a unique and universal drought index that could integrate all the critical data required to assess drought and give realistic information about drought severity.[3] To characterize drought with a single index is not sufficient. Identifying rainfall as the single most important factor responsible for initiating drought conditions, the World Meteorological Organization recommended a standardized precipitation index (SPI) to be used by all national meteorological and hydrological services for monitoring droughts at various time scales.[4] Various studies have shown variation of SPI in response to soil moisture, river discharge, reservoir storage, vegetation activity, crop production, and piezometric fluctuations at different time scales.[16–20] However, one of the drawbacks in SPI is that it does not take into account variation of other climatological parameters such as temperature, wind speed, and evapotranspiration. Abramopoulos et al.[21] and Vicente-Serrano[18] reported that temperature rise can significantly affect drought severity and evapotranspiration can consume up to 80% of rainfall. During the past 150 years, there has been a general temperature increase (0.5°C to 2°C), and climate change models predict a significant increase during the 21st century.[22] It is estimated that this temperature rise will have drastic consequences for drought severity conditions, with increase in water demand due to evapotranspiration.[22] Vicente-Serrano et al.[2] suggested the use of the standardized precipitation and evapotranspiration index (SPEI) based on monthly rainfall and air temperature data to analyze variability of temperature along with rainfall for detecting, monitoring, and exploring consequences of temperature variability on vegetation and drought conditions. SPEI is also a multiscalar drought index and incorporates changes in potential evapotranspiration (PET) caused by temperature fluctuations.

Remotely sensed NDVI forms a robust index, extracted from directly observed vegetation satellite data, for monitoring wet as well as drought conditions. NDVI and NDVI anomalies have been extensively used for drought assessment and vegetation change dynamics along with meteorological drought indices.[23–29] However, NDVI anomalies do not allow easier and meaningful profile comparison with SPI and SPEI. This is due to the fact that both SPI and SPEI are standardized and generated a value around zero after incorporating the effect of long-term data as against NDVI or NDVI anomalies. This study incorporated the standardized vegetation index (SVI) developed by Peters et al.,[30] for drought monitoring across the central part of the United States. It is a simple index and generates SVI values around means such as SPI and SPEI. SVI allowed meaningful profile comparison with meteorological drought indices (SPI and SPEI) and furnished critical insight into variability of vegetation data in response to variations in rainfall and temperature across the arid region of Tharparkar.

Drought indices give separate pictures of drought severity across the study area based on input data of drought indices. Information from all variables is needed on one layer to generate a composite picture of drought hazard across the study area. Weighted overlay analysis in geographical information systems (GIS) provides a method to generate composite response of drought hazard and gives a clear picture of drought severity by emphasizing common information from all drought indices brought on equal scale. Shaheen and Baig[16] used weighted overlay analysis to generate composite drought hazard maps at meteorological and agricultural scale in the arid region of Thal Doab, Pakistan. Shahid et al.[31] generated composite drought hazard maps for Bangladesh using different drought monitoring indices. This study used drought severity layers of SPI, SPEI, and SVI to generate composite drought hazard maps at meteorological and agricultural scale through weighted overlay analysis in GIS.

The objective of this study is to perform spatial–temporal analysis of vegetation dynamics and drought severity across the arid region of Tharparkar using remote sensing-derived indices. The study included analysis of vegetation dynamics, analysis of meteorological and agricultural droughts, and modeling of drought severity across Tharparkar, using SPI, SPEI, and SVI through weighted overlay analysis in GIS. The results of this study presented an effective model for drought severity analysis across data-scarce arid regions to aid in drought preparedness and response.

2 Data

2.1 *Study Area*

Tharparkar is a desert region and classified as an arid climate in the southeastern part of Sindh province, Pakistan (Fig. 1). Tharparkar is an extension of the Indian arid zone of Rajasthan on the eastern border of Pakistan. The study area lies between 69°E and 29°N to 71°E and 24°N. It consists of five subregions, i.e., Chachro, Diplo, Mithi, Nagarparkar, and Umarkot, with total area of 27,135 km^2 and a population of about 1.5 million. Tharparkar, being a remote area of Sindh province, remains disadvantaged with low indicators of education and health while recurring droughts making life more difficult.[32,33]

Tharparkar has a tropical climate with min temperatures during winters in December and January (4°C to 6°C] while max temperature ranges from 38°C to 41°C during the summer. Tharparkar consists of homogeneous topography with predominantly sandy terrain and faces spatial variability in rainfall from east to west mainly associated with relief of the area.[34]

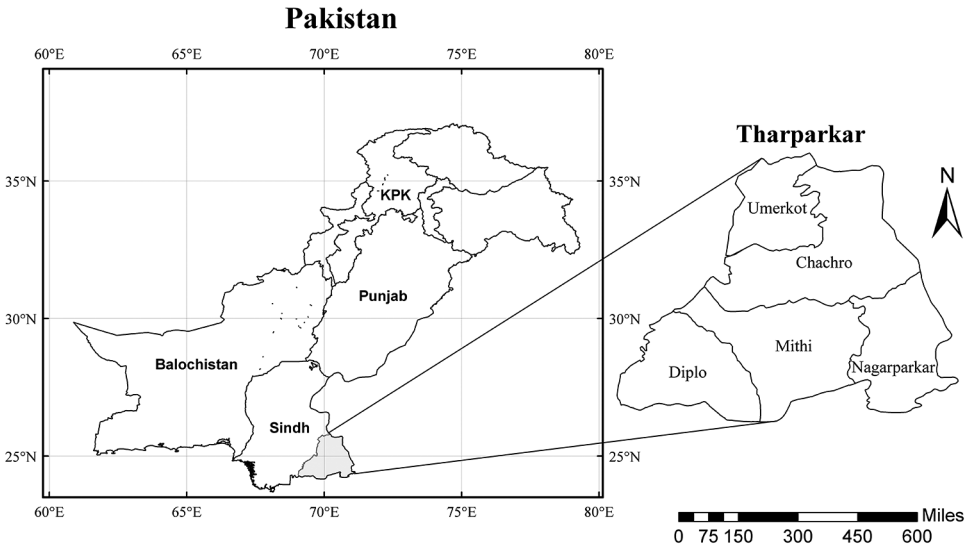

Fig. 1 Study area.

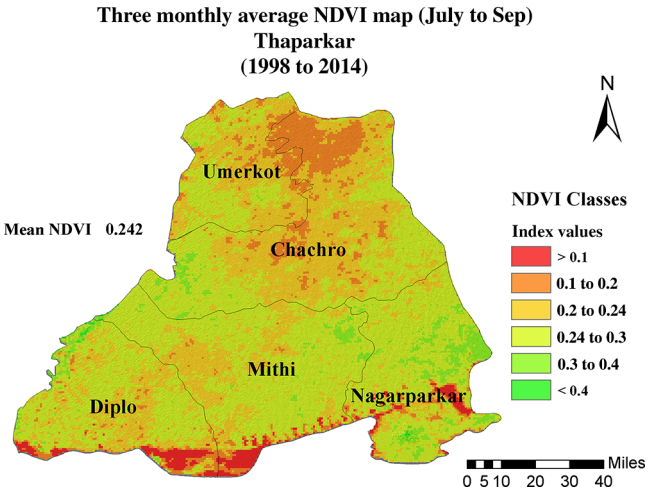

Fig. 2 Average NDVI depicting average vegetation across Tharparkar from July to September (2000 to 2014).

The sandy nature of soil, higher temperatures, lack of surface water resources, and mostly brackish underwater resources allow rain-fed agriculture and livestock to be the only source of livelihood for Thari people. Both of these sources of income depend directly or indirectly on monsoon rainfall in the monsoon season from June to September.[32,35] The main crops of Tharparkar are cluster beans, guar seed, millet, pulses, and fodder. The vegetation consists mostly of scattered scrub and bush. The ground cover is provided by patches of grasses used as a fodder for the livestock. Higher rates of evaporation and absence of surface water resources aggravate problems for the already fragile agro-ecosystem. It was predicted by Goyal[34] that an increase in temperature in this region would aggravate drought severity. Average NDVI data of Tharparkar from July to September for the study period depicted that south, southeastern, and most of the area on the eastern border remained above mean NDVI. While the central and northern part of Tharparkar, comprising most of the area in Chachro and Umerkot, remained below mean NDVI (Fig. 2).

2.2 *Observed Rainfall and Air Temperature Data*

Processed monthly rainfall and air temperature data (max and min) were acquired from the Pakistan Meteorological Department (PMD) at two met observatories, i.e., Chor and Badin (Fig. 4). However, the monthly rainfall data acquired from PMD could not provide spatial variability of precipitation over the study area, which was necessary to map and analyze spatial and temporal variability of drought across the study area. Air temperature having a strong relation with topography of the area varies with a lapse rate of −0.98°C for dry air to about −0.4°C for saturated dry air with each 100 m rise in altitude.[36] Tharparkar has a homogeneous topography with altitude variation of only 170 m across the entire area except in the southern part of Nagarparkar where in the small hills range (19 km) altitude varies to 305 m. The inverse distance weighted (IDW) method works well with air temperature interpolation in homogeneous and relatively flat terrain.[36] IDW interpolates the unknown values within the max and min observed data ranges, i.e., it does not extrapolate beyond its range and is mostly used for interpolation of meteorological data.[37] Luzio et al.[38] constructed precipitation and temperature datasets for the conterminous United States and found that simple IDW provided reasonable results in situations where they had low spatial density of stations. Yang et al.[39] used four interpolation techniques to produce finer resolution rainfall datasets over the greater Sydney region and found that IDW gave best results as compared to other methods. Thus, the observed air temperature at Chor and Badin was interpolated using IDW to achieve spatial variation of temperature across the study area. It was also observed that yearly mean temperature across Tharparkar also started rising from 2006 (Fig. 3).

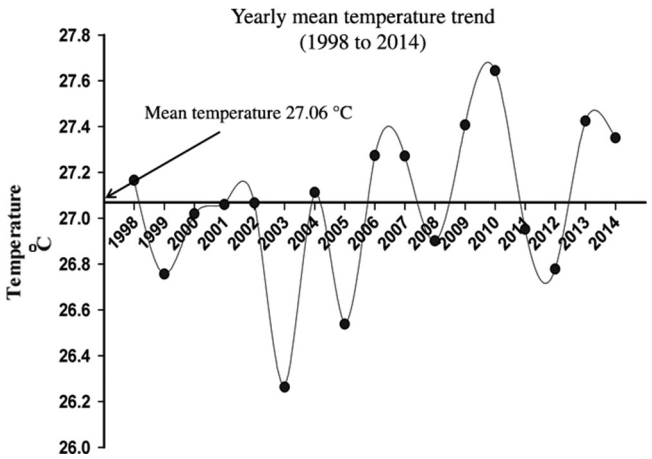

Fig. 3 Yearly mean temperature trend from 1998 to 2014.

2.3 *TRMM (3B43) Monthly Rainfall Dataset*

To achieve spatial and temporal variability of rainfall across the study area, TRMM 3B43 multi-satellite precipitation analysis products were used to extract monthly precipitation data from 1998 to 2014. TRMM precipitation is a combination of datasets from visible and infrared (IR) scanners, a special sensor microwave imager, a microwave imager, a precipitation radar, and a global precipitation climatology center rain gauge data available at 0.25 deg ×0.25 deg spatial resolution. The TRMM 3B43 algorithm combines 3-h integrated high-quality data and IR estimates (3B42) with the monthly accumulated climate assessment monitoring system.[40] The data were downloaded from Ref. 41. Estimated TRMM 3B43 monthly rainfall data were initially correlated with observed monthly precipitation data at Chor and Badin to check feasibility for using TRMM 3B43 datasets across the study area. Estimated TRMM 3B43 rainfall data obtained significant correlation with observed precipitation data as shown in Fig. 4. The scatter plot exhibited that the TRMM data were in general agreement with gauge data at lower values. At higher values, TRMM overestimated data at Badin but generally remained near the gauge data at Chor. Root-mean-square error (RMSE) at both met observatories remained constant at 18 and 19 mm. RMSE was 5.6% of the max observed gauge value at Badin and 4.7% of the max observed gauge value at Chor. The TRMM (3B43) monthly datasets were used for the entire time series; therefore, consistency of utilizing the same data gave relative temporal estimates through the same algorithm and hence was not critical.

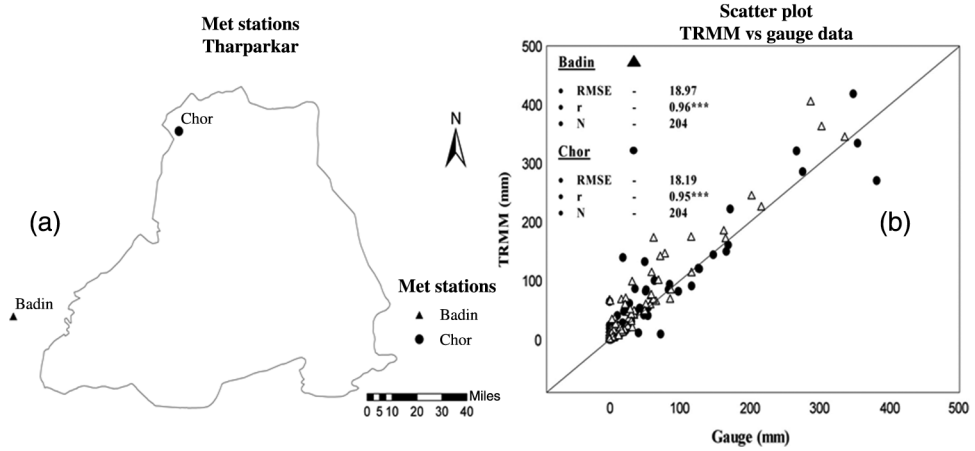

Fig. 4 (a) Location of met observatories at and near Tharparkar and (b) scatter plot between gauge and TRMM data at Chor and Badin, showing significant correlation between TRMM and gauge data.

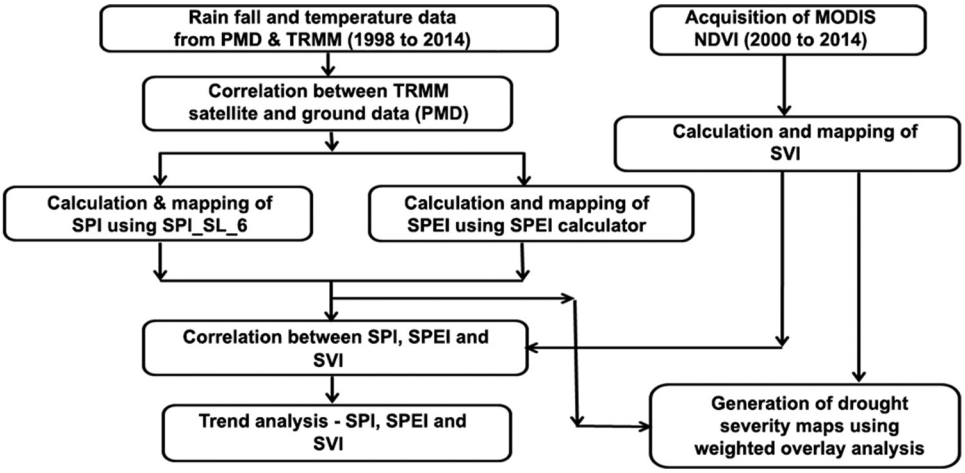

Fig. 5 Research methodology.

2.4 *MOD13A3 1 km Monthly NDVI Dataset*

Global MODIS vegetation indices provide continuous temporal and spatial information about vegetation conditions.[42] The MODIS 1-km MOD13A3 VI NDVI images were used to calculate one-monthly, three-monthly, and six-monthly SVI. The monthly 1-km MOD13A3 VI product is generated using the 16-day 1-km MODIS VI output using a temporal compositing algorithm based on a weighted average scheme to create a calendar-month composite.[43] MODIS images were downloaded from Ref. 44.

3 Methods

The methodology adopted for the study has been highlighted in Fig. 5. Grid points were generated across the study area to extract TRMM 3B43 monthly rainfall data at these points.

Grid points were generated with a view to have equal spacing among the grid points; however, grid points were added and adjusted to account for the spatial variation of precipitation across the study area as shown in Fig. 6. Monthly rainfall amounts at these grid points were extracted from the TRMM 3B43 datasets while the monthly mean air temperatures were

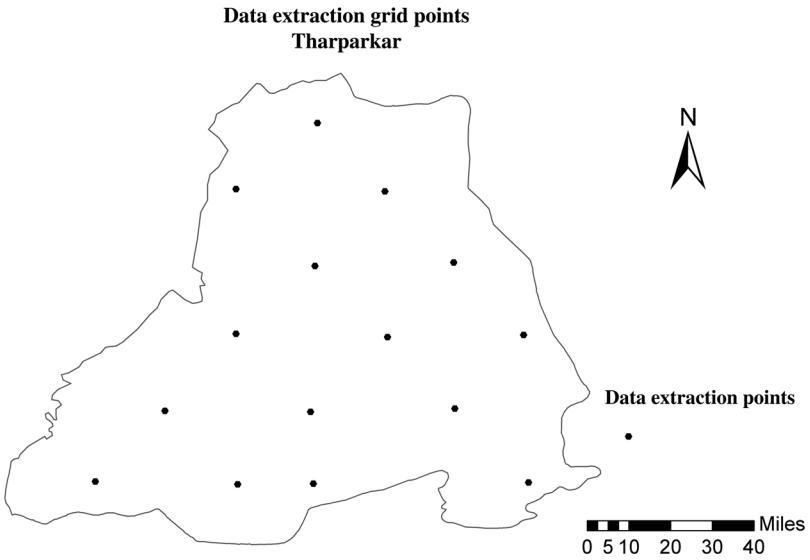

Fig. 6 Grid points generated for data extraction from TRMM monthly rainfall satellite data and interpolated monthly air temperature data at Chor and Badin.

extracted from interpolated observed monthly mean air temperature data from two met observatories, i.e., Chor and Badin.

3.1 *Calculation and Mapping of Standardized Precipitation Index*

The SPI at grid points was calculated using the SPI computer program, SPI_SL_6.exe, downloaded from Ref. 45, with input files generated at each grid point using monthly mean rainfall amounts. SPI at a location is found by a series of equations as below. Precipitation time series at a location was found to fit gamma distribution well by Thom.[46] The probability density function defined gamma distribution for $x > 0$

$$g(x) = \frac{1}{\beta^{\alpha}\Gamma(\alpha)} x^{\alpha-1} e^{-\frac{x}{\beta}}, \tag{1}$$

where α is a shape, β is a scale parameter, x is a precipitation, and $\Gamma(\alpha)$ is a gamma function and

$$\alpha = \frac{1}{4A}\left(1 + \sqrt{1 + \frac{4A}{3}}\right),$$

$$\beta = \frac{\bar{x}}{\alpha}, \tag{3}$$

$$A = \ln\,(\bar{x}) - \frac{\sum \ln\,(x)}{n}, \tag{4}$$

and n is the number of observations. The cumulative probability of the observed precipitation is found as follows:

$$H(x) = q + (1 - q)G(x), \tag{5}$$

where q is a probability of zero $G(x)$.[1] This probability is converted to the standard normal random variable Z, which is the SPI index value. One-monthly, three-monthly, and six-monthly SPI layers were generated for the study area using IDW in ArcGIS 10.1.

3.2 *Calculation and Mapping of Standardized Precipitation and Evapotranspiration Index*

The SPEI at the grid points was calculated using the SPEI calculator available at Ref. 47. Mathematically, SPEI is similar to the SPI but includes the role of temperature and latitude of location to calculate PET at a particular location. Calculation of PET is a complicated task and, based on data availability, different methods have been proposed for PET estimation from meteorological parameters. The two main approaches for PET calculation are: physically based methods [the Penman—Monteith method (PM)] and methods based on models that use empirical relationships where PET is calculated with sparse data. The PM method is currently being used as standard procedure for PET calculation by the Food and Agriculture Organization, the International Commission for Irrigation, and the American Society of Civil Engineers.[6] The PM method needs a large amount of data including relative humidity, temperature, solar radiations, and wind speed for its calculation. This type of meteorological data is generally not available in most of the world as in our case of Tharparkar. To overcome this limitation, empirical equations have been developed to calculate PET where there is a lack of data.[6] Although some methods give better PET results than others,[48] the aim of including PET in a drought index is to get relative temporal estimation and therefore the method used to estimate PET is not critical.[2] Mavromatis[49] showed that the method used to calculate PET, may it be simple or complex, gives similar results when used in a multiscalar drought index. Therefore, we followed the Thornthwaite (1948) method to calculate PET as we had only monthly mean temperature data available, which offers advantage of using only monthly mean temperature data for PET calculation. One-monthly, three-monthly, and six-monthly SPEI layers were generated for the study area using IDW in ArcGIS 10.1.

3.3 *Calculation and Mapping of Standardized Vegetation Index*

For ease of comparison and correlation analyses, NDVI anomalies were standardized by variability of data. The resulting SVI value was a deviation from zero value identical to SPI and SPEI. SVI was calculated using the following:

$$\mathrm{SVI} = \frac{\mathrm{NDVIi} - \mathrm{NDVImean}}{\sigma},$$

where SVI is a deviation from the long-term mean. NDVIi is a current NDVI value, NDVI mean is a long-term mean, and σ is a standard deviation of the long-term NDVI values. One-monthly, three-monthly, and six-monthly SVI layers were generated for the study area by processing NDVI layers through Raster Calculator in ArcGIS 10.1.

3.4 *Correlation Between Drought Indices and Weighted Overlay Analysis*

Three-monthly SPI, SPEI, and SVI were generated for three critical months of July to August, which receive maximum rainfall to characterize meteorological drought conditions during each year. Six-monthly SPI, SPEI, and SVI were generated from May to October each year to characterize agricultural drought conditions during each year. Monthly drought indices were also generated from June to October during each year to perform correlation analysis among three indices to characterize the relationship of rainfall and temperature data with vegetation across the study area.

United States drought monitor values for SPI were used for classification of both SPI and SPEI maps. Classification values are available at Ref. 50 and SVI values are available at Ref. 51, which were used with slight modification for classification of SVI maps as shown in Table 1.

For weighted overlay analysis, SVI was given first priority while assigning weights, being a direct estimation of vegetation data followed by SPEI and SPI, which was based on correlation analysis among SPI, SPEI, and SVI. Weights between prioritized drought index layers were calculated and balanced through an analytic hierarchy process program with a consistency ratio of less than 10%.[52] All the drought index layers were generated on 1-km spatial resolution to make layers of three drought indices compatible for weighted overlay analysis in ArcGIS. Drought severity classes in all the layers as given in Table 1 were scaled on a common scale of 1 to 9 with 1 for severely wet and 9 for exceptional drought. Weighted overlay analysis was completed in ArcGIS with SPI, SPEI, and SVI layers to generate meteorological and agricultural drought severity maps for Tharparkar.

Table 1 Drought classification values of SPI, SPEI, and SVI.

Drought classification	SVI	SPI	SPEI
Exceptional drought	≥ −2	≥ −2	≥ −2
Extreme drought	−1.5 to −2	−1.6 to −1.9	−1.6 to −1.9
Severe drought	−1 to −1.5	−1.3 to −1.5	−1.3 to −1.5
Moderate drought	−0.5 to −1	−0.8 to −1.2	−0.8 to −1.2
Abnormally dry	−0.1 to −0.5	−0.5 to −0.7	−0.5 to −0.7
Normal	0.1 to −0.1	—	—
Wet	0.1 to 1	—	—
Moderately wet	1 to 1.5	—	—
Severely wet	≤1.5	—	—

4 Results

4.1 *Average Vegetation Change in Response to Average Rainfall Variations*

Monsoon season in Tharparkar spans from June to October each year with corresponding response from the vegetation cover. Monsoon season starts in June, ascending to peak in July or August, and finally ends in October. Vegetation in Tharparkar reciprocates to the time and amount of monthly rainfall during monsoon season by conforming to corresponding monthly NDVI response as exhibited by monthly rainfall. Other months receive little to no rainfall events without any pattern. Figures 7(a) and 7(b) show average monthly rainfall and average monthly NDVI from 1998 to 2014, respectively. Average monthly rainfall marks the optimum monthly rainfall pattern across Tharparkar for the time period from 1998 to 2014 and creates a threshold of monthly rainfall for optimum growth of vegetation types across Tharparkar.[53–55] Average monthly NDVI pattern also exhibited that after each monsoon season NDVI response diminishes gradually from November through May the following year with the lowest NDVI in May. NDVI gradually sustains itself during a cycle of no rainfall between two monsoon seasons, coming to lowest level before the start of the next monsoon season. Thus, the vegetation condition that extends to the next monsoon season plays its role in the carryover effect of drought conditions to the next season.

4.2 *Correlation Analysis—Vegetation Response to Rainfall Variations*

Table 2 shows the correlation coefficient pattern among SPI, SPEI, and SVI from 1998 to 2014. Correlations of SPI and SPEI with SVI varied from significant correlation in June to highly significant correlation in July. Correlation decreased after its peak in July to strong significant correlation in August and September before reducing to no correlation in October. Correlation between SPI and SPEI remained highly significant from June to September before decreasing to significant correlation. Correlation configuration of SPI and SPEI with SVI implied that vegetation gave the strongest response to monthly rainfall during July, followed by August. Thus, the time and amount of monthly rainfall from June to October played a vital role for the vegetation growth cycle during the monsoon season across Tharparkar. Correlation analysis of SPI and SPEI with SVI implied that vegetation was adapted to time and amount of monthly rainfall across the arid zone of Tharparkar.[14,53] Correlation configuration between SPI and SPEI suggested that the moisture loss due to evapotranspiration did not become significant for months that received higher rainfall; however, correlation difference between SPI and SPEI increased for months that received lesser rainfalls.

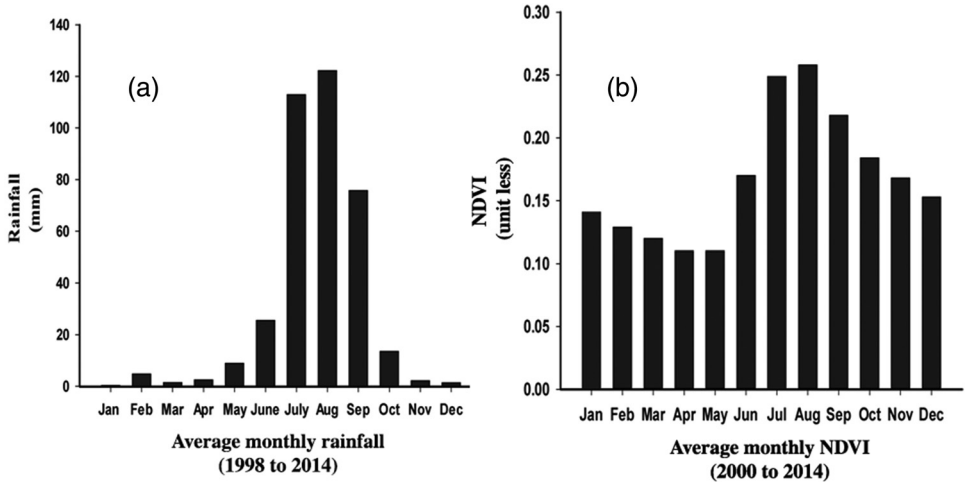

Fig. 7 Average monthly rainfall versus average monthly NDVI: (a) average monthly rainfall and (b) average monthly NDVI.

Table 2 Correlation coefficient values (r) between SPI, SPEI, and SVI from 1998 to 2014.

Duration	SVI versus SPI ($N = 15$)	SVI versus SPEI ($N = 15$)	SPI versus SPEI ($N = 17$)
Jun.	0.46[a]	0.58[a]	0.80[c]
Jul.	0.81[c]	0.81[c]	0.96[c]
Aug.	0.71[c]	0.73[c]	0.95[c]
Sep.	0.64[b]	0.68[c]	0.83[c]
Oct.	−0.0056	0.02	0.46[a]
Three-monthly correlation (Jul. to Sep.)	0.87[c]	0.88[c]	0.95[c]
Six-monthly correlation (May to Oct.)	0.85[c]	0.80[c]	0.93[c]

[a]Significant at 0.05 probability level.
[b]Significant at 0.01 probability level.
[c]Significant at 0.001 probability level.

4.3 *Vegetation Dynamics—Normal, Near Normal, and Wet Years*

Tharparkar experienced normal, near normal, or wet conditions during 1998, 2001, 2003, and 2006 to 2013. 1998, 2003, 2006, 2010, 2011, and 2013 were wet years with rainfall above normal (371 mm) during the monsoon season while 2001, 2007, 2008, 2009, and 2012 received comparatively less than normal rainfall and faced normal or near-normal conditions (Fig. 8).

4.3.1 *Vegetation response dynamics—normal and near-normal years*

Tharparkar faces high spatial and temporal variability of rainfall alongside very high temperatures during the monsoon season with maximum temperature ranging from 35°C to over 40°C.[32]

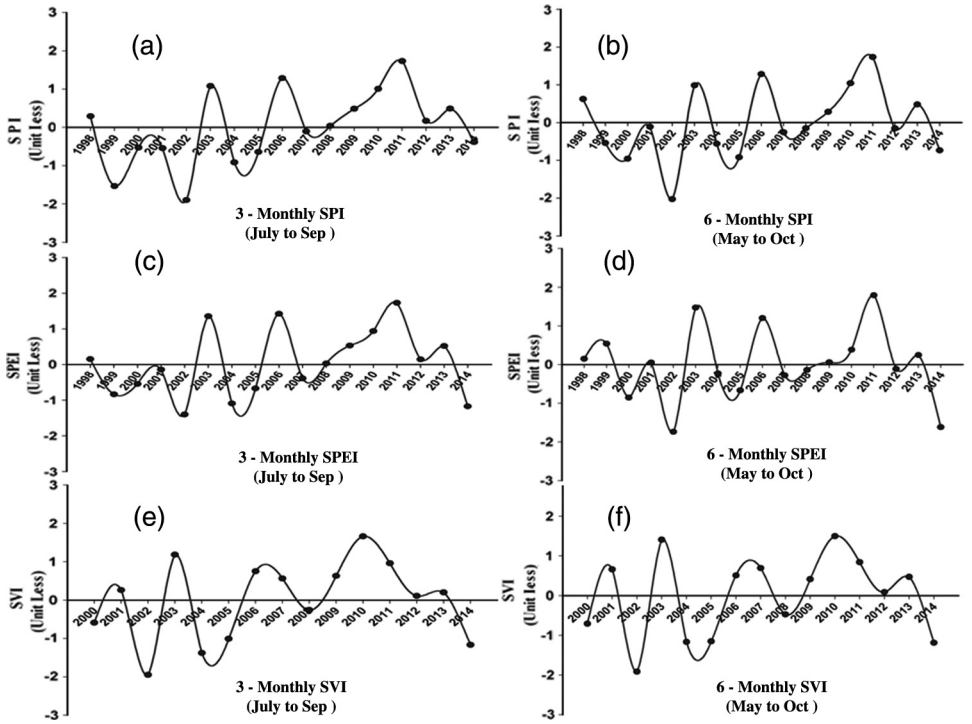

Fig. 8 Temporal variation of drought indices: (a) three-monthly SPI, (b) six-monthly SPI, (c) three-monthly SPEI, (d) six-monthly SPEI, (e) three-monthly SVI, and (f) six-monthly SVI.

For optimum or maximum growth of vegetation, it was essential for rainfall to follow an optimum or more than optimum pattern of rainfall during the complete monsoon season across Tharparkar. Absence or lower than normal rainfall during any of the months while accompanied by high-temperature anomalies badly affected the vegetation growth cycle and reduced overall NDVI response at the end of the monsoon season.[14] During 2001, the monthly rainfall pattern initiated on time in June, with higher than normal monthly rainfall during June, but lasted up to August only with lower than normal rainfall both in July and August. Lower than normal rainfall during July and August (Table 3), while positive monthly temperature anomalies in September and October, resulted in negative NDVI anomalies during August, September, and October reducing overall response of vegetation across Tharparkar. Thus three- and six-monthly drought indices indicated normal values for 2001 (Fig. 8).

Tharparkar experienced normal conditions continuously from 2007 till 2009 after wet conditions in 2006 (Fig. 8). During 2007, monthly rainfall varied with alternatively higher than normal rainfall in June and August while there was lower than normal rainfall during July, September, and October. Lower rainfall in July, September, and October, together with higher monthly temperature anomalies in September and October, resulted in normal conditions at meteorological and agricultural drought scale. Monthly NDVI anomaly attained maximum value in July 2007 but decreased sharply in August 2007 (Table 3).

Although monsoon season in 2008 almost received analogous monthly rainfall and air temperature anomalies pattern as in 2007, three- and six-monthly SVI indicated lower than normal values for 2008 (Fig. 8). This contradiction was explained by the carryover effect of vegetation condition from one monsoon season to another. After a wet year of 2006, monthly NDVI anomalies from November 2006 till May 2007 remained positive while monthly NDVI anomalies were negative in May 2008 (Table 3), thus imparting an additive effect to slightly dry conditions during the monsoon season in 2008. This phenomenon repeated as the monsoon season of 2009 approached, which received more than normal rainfall during the monsoon season but yet produced three- and six-monthly NDVI anomalies almost the same as in 2007 (Fig. 8).

4.3.2 *Vegetation response dynamics—wet years*

Wet years received over 450 to 731 mm of rainfall during monsoon seasons. Although rainfall quantity was well above normal rainfall (371 mm) during wet years in monsoon seasons, SVI response varied between wet years due to variations in monthly rainfall distributions. The 2011 (731 mm) and 2006 (617 mm) were the wettest years in terms of total amount of rainfall yet SVI exhibited peak values in 2003 and 2010 signifying that 2003 (534 mm) and 2010 (544 mm) were the most green years (Fig. 8). This variation in response of SVI was explained by monthly rainfall variations during the monsoon season when compared with the optimum monthly rainfall pattern for Tharparkar from 1998 to 2014 (Fig. 9).

The 2003 and 2010 were the only two wet years during which July and August received highest rainfalls in sequence (Table 4). In addition, 2010 was the only year when the monthly rainfall pattern during monsoon perfectly followed the optimum configuration of rainfall from June until September and resulted in the highest SVI during the complete time series (Fig. 9).

Although 2006 and 2011 received the highest monsoon rainfalls, the monthly rainfall pattern did not conform well to the optimum monthly configuration of rainfall during July and August as in 2003 and 2010 (Fig. 9). Rainfall pattern during 2013 received well over the normal monthly rainfall during the entire monsoon season except for the critical month of August (Table 4), thus impeding the vegetation growth cycle during the significant month of August and resulted in lower SVI (Fig. 8).

4.3.3 *Temperature anomalies variations—wet and normal years*

The greenest years across Tharparkar, i.e., 2003 and 2010, had an opposite pattern of temperature anomalies during monsoon seasons. The 2003 experienced low negative temperature anomalies during the entire monsoon season, whereas 2010 experienced high positive temperature anomalies during the entire monsoon season except August (Table 4). Monthly rainfall remained the dominating factor for vegetation growth cycle as long as the amount of monthly

Table 3 Monthly rainfall, monthly NDVI anomalies, and monthly temperature anomalies for normal years.

Year	Monthly data	Jan.	Feb.	Mar.	Apr.	May	Jun.	Jul.	Aug.	Sep.	Oct.	Nov.	Dec.
2001	Monthly rainfall (mm)	0	0	0	5	13	111	103	73	10	7	0	0
	Monthly NDVI anomalies	−0.022	−0.019	−0.019	−0.020	−0.020	0.144	0.070	−0.002	−0.017	−0.005	0.004	0.008
	Monthly temperature anomalies	−0.491	−0.148	−0.172	−0.358	0.509	−0.603	−1.540	−0.079	0.130	1.247	0.282	1.246
2007	Monthly rainfall (mm)	0	16	7	0	2	35	81	132	41	0	0	6
	Monthly NDVI anomalies	0.032	0.021	0.022	0.020	0.026	0.037	0.075	0.019	0.016	0.006	0.006	0.003
	Monthly temperature anomalies	0.697	2.234	−0.768	0.628	−0.167	−0.202	0.113	0.552	0.897	−0.928	0.475	−0.972
2008	Monthly rainfall (mm)	0	1	1	10	1	25	97	140	45	0	1	12
	Monthly NDVI anomalies	0.002	0.004	0.001	0.000	−0.002	−0.053	−0.006	−0.026	−0.018	−0.016	−0.01	−0.012
	Monthly temperature anomalies	−1.485	−2.254	1.228	−0.511	−0.367	−0.168	0.147	−0.494	0.696	0.510	−0.151	0.971
2009	Monthly rainfall (mm)	2	0	0	0	0	11	296	69	11	0	0	0
	Monthly NDVI anomalies	−0.014	−0.012	−0.011	−0.010	−0.011	0.004	0.070	0.057	−0.004	−0.009	−0.007	0.000
	Monthly temperature anomalies	1.384	1.717	1.083	0.019	0.616	0.379	0.326	0.219	−0.388	−0.475	−0.815	0.127
2012	Monthly rainfall (mm)	0	0	0	3	0	1	34	88	184	0	0	1
	Monthly NDVI anomalies	0.020	0.015	0.018	0.019	0.018	−0.041	−0.073	0.040	0.054	0.025	0.021	0.012
	Monthly temperature anomalies	−0.266	−2.154	−0.924	−0.093	−0.101	−0.104	0.260	0.591	−0.407	−0.513	−0.097	0.459

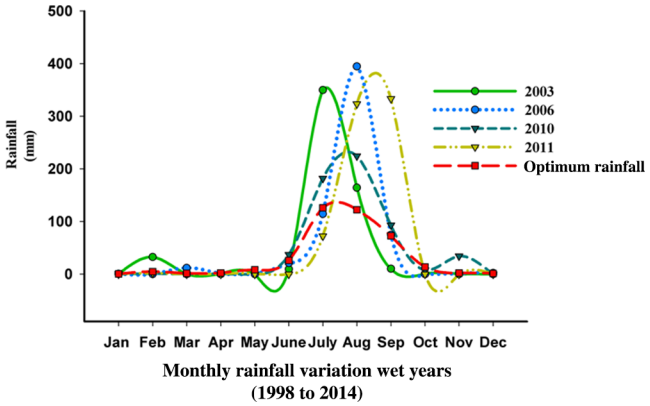

Fig. 9 Comparison of monthly rainfall variations versus optimum monthly rainfall during wet years.

rainfall remained above optimum quantity during a particular month of monsoon season without any influence of temperature rise. However, significant lower monthly rainfall during any of the months of the monsoon season coupled with high positive temperature anomalies badly affected vegetation growth cycle and reduced overall vegetation response at agricultural scale, e.g., in August 2000, August 2004, June 2009, June 2011, July 2012, and during a complete drought year of 2014, which have been discussed in detail in Sec. 4.4.2.

4.4 *Temporal and Spatial Variation of Drought Intensity Across Tharparkar*

Tharparkar faced droughts during 1999, 2000, 2002, 2004, 2005, and 2014 over the period under study and saw either near-normal or wet conditions during the remaining period. Impact of variation in rainfall and temperature on drought intensity was evaluated through analysis on temporal and spatial variations of drought indices across Tharparkar.

4.4.1 *Impact of rainfall and temperature on temporal variations of drought intensity across Tharparkar*

Tharparkar faced severe meteorological drought during 1999 triggered by very low rainfall during the critical months of July to September. Three-monthly SPI exhibited (−1.53) extreme meteorological drought while three-monthly SPEI indicated (−0.83) moderate meteorological drought; however, six-monthly SPI (−0.54) and SPEI (0.54) depicted abnormally dry and normal conditions. Meteorological drought in 1999 was mainly initiated due to very low rainfall during the three critical months from July to September; however, intensity of drought was reduced due to late season rainfall in October (46 mm) and low monthly temperatures during the monsoon season as illustrated by significant negative temperature anomalies (Table 5). Negative temperature anomalies also resulted in depicting low intensity of drought by SPEI as against SPI. Contrary to 1999, drought in 2000 started with low meteorological drought severity as SPI (−0.53), SPEI (−0.55), and SVI (−0.59) exhibited abnormally dry conditions. However, agricultural drought severity was increased to moderate drought as displayed by all drought indices (Fig. 8). This was explained through monthly rainfall variations during the monsoon season in 2000 as the monsoon season only received normal rainfall during July and low rainfall during August but other months did not receive any or appreciable rainfall causing an increase in agricultural drought severity. Monthly temperature anomalies during the monsoon season in 2000 remained near-normal values (Table 5), thus SPI, SPEI, and SVI exhibited approximately similar values without showing any dissimilarity in drought intensity.

SPEI exhibited low drought intensity when monthly temperature anomalies were negative in 1999 and depicted almost the same drought intensity as SPI during 2000 when monthly temperature anomalies were around normal values. Tharparkar faced extreme to exceptional drought in 2002 with a very small amount of rainfall in June (34 mm) and August (22 mm) while other months received no or little rainfall. Monthly temperature anomalies remained at normal during

Table 4 Monthly rainfall, monthly NDVI anomalies, and monthly temperature anomalies for wet years.

Year	Monthly data	Jan.	Feb.	Mar.	Apr.	May	Jun.	Jul.	Aug.	Sept.	Oct.	Nov.	Dec.
1998	Monthly rainfall (mm)	0	6	3	0	0	34	61	73	201	89	0	0
	Monthly NDVI anomalies	No data	No data	No data	No data	No data	No data	No data	No data	No data	No data	No data	No data
	Monthly temperature anomalies	−0.023	−0.566	−0.940	0.742	0.695	0.652	−0.150	0.729	0.713	−0.205	−1.148	0.791
2003	Monthly rainfall (mm)	0	32	0	0	0	9	350	164	10	0	0	0
	Monthly NDVI anomalies	−0.043	−0.020	−0.010	−0.015	−0.016	0.124	0.098	0.109	0.022	0.025	0.029	0.038
	Monthly temperature anomalies	0.191	0.114	−0.506	−0.577	−0.693	−0.398	−0.566	−0.58	−1.243	−0.982	−2.803	−1.495
2006	Monthly rainfall (mm)	0	0	12	1	0	21	114	395	74	0	0	2
	Monthly NDVI anomalies	−0.020	−0.021	−0.024	−0.024	−0.021	−0.025	0.037	0.055	0.053	0.032	0.031	0.026
	Monthly temperature anomalies	−0.146	3.614	−0.755	−0.088	0.353	0.299	0.379	−1.43	−0.155	0.743	0.157	−0.384
2010	Monthly rainfall (mm)	0	1	0	0	0	37	182	224	93	8	34	0
	Monthly NDVI anomalies	−0.003	−0.006	−0.009	−0.008	−0.004	0.021	0.097	0.139	0.087	0.047	0.027	0.020
	Monthly temperature anomalies	0.707	0.278	2.715	1.616	1.571	0.147	0.615	0.336	0.078	0.707	−0.365	−1.374
2011	Monthly rainfall (mm)	1	2	0	0	0	0	72	323	333	0	0	0
	Monthly NDVI anomalies	0.018	0.015	0.012	0.011	0.008	−0.027	0.037	0.080	0.069	0.050	0.037	0.029
	Monthly temperature anomalies	−0.494	0.027	0.228	−1.212	−0.521	0.148	0.496	−0.30	−1.709	−0.477	2.063	0.478

June and August while remaining negative during July and September. Owing to normal or negative temperature anomalies during the monsoon season, SPEI indicated severe meteorological and extreme agricultural drought while both SPI and SVI demonstrated severe to exceptional meteorological and agricultural drought conditions. Hence, SPI matched drought intensity of SVI generated from vegetation data during 2002 while SPEI depicted lower drought severity due to lower monthly temperature anomalies. Tharparkar faced droughts consecutively during 2004 and 2005. Although rainfall season of 2004 received more rain as compared to 2005 still drought intensity as indicated by SVI was more as compared to 2005 (Fig. 8). There were two prominent reasons for this difference, one was lower monthly rainfall during critical months from July to September and another was higher positive monthly air temperature anomalies during the rainfall season of 2004 as compared to 2005 (Table 5).

From 2006 till 2013, Tharparkar either experienced normal or wet conditions till 2013. After 2005, Tharparkar faced drought conditions in 2014. From 2006 till 2013, Tharparkar came across either normal or near-normal conditions as in 2007 and 2008, or very wet meteorological conditions as in 2010 and 2011 during critical months of the monsoon season.

4.4.2 *Effect of rise in temperature on drought intensity across Tharparkar during 2014*

Monthly rainfall variations in monsoon seasons of 2005 and 2014 presented an ideal case to illustrate the effect of rise in temperature on drought severity during 2014 due to two significant reasons. Despite the fact that the monsoon season in 2014 not only received more rainfall than the monsoon season of 2005 and monthly rainfall pattern during 2014, but also followed more closely to optimum rainfall pattern from July to September as against 2005, yet SVI displayed more drought severity in 2014 than 2005 (Fig. 8). This contradiction was explained well by SPEI and temperature anomalies during rainfall seasons of 2005 and 2014. The effect of rise in temperature was indicated by comparison of statistical variations in areas of drought severity classes.

Table 6 shows areas covered, in terms of percentage, with drought severity classes by three drought indices during droughts in 2005 and 2014. SPI displayed more area under higher drought classes in 2005 as against drought year of 2014 at both meteorological and agricultural drought levels. SPI showed more drought severity in 2005 compared to 2014 while SPEI and SVI exhibited more areas under higher drought severity classes specifically under severe and extreme drought classes, respectively, at both meteorological and agricultural drought levels. This inconsistency was explained by temperature anomalies during rainfall season, which were highest for monsoon season months during 2014 for the entire study period (Table 5). The effect of the rise in temperature coupled with lower rainfall during the monsoon season was adequately taken into account by SPEI and SVI while SPI could not incorporate the effect of rise in temperature.[2]

4.5 *Spatial Variation of Meteorological and Agricultural Drought Severity Across Tharparkar During Drought Years*

Drought indices gave a reasonable display of spatial variation of areas affected by type of drought severity classes across Tharparkar (Figs. 10 and 11) but any single variable could not incorporate important information from other variables. In case of the drought year of 2014, while SPI depicted less drought severity than SVI, SPEI showed more drought severity than SVI. In order to get composite maps at both meteorological and agricultural drought scales with optimum scalable information fused from all drought indices, weighted overlay analysis in ArcGIS was done. Composite drought severity maps for drought years of 2002, 2005, and 2014 as shown in Fig. 12 gave very clear representation of areas affected by drought severity classes across Tharparkar. Weighted overlay analysis emphasized information of drought severity classes contained in three drought index layers and furnished clear information about areas affected by respective drought severity classes across Tharparkar at both meteorological and agricultural drought scales (Fig. 12).

Meteorological drought severity map for 2014 exhibited the northern area of Mithi, central and northeastern areas of Chachro, southern part of Umerkot, and central area of Nagarparkar

Table 5 Monthly rainfall, monthly NDVI anomalies, and monthly temperature anomalies for drought years.

Year	Monthly data	Jan.	Feb.	Mar.	Apr.	May	Jun.	Jul.	Aug.	Sept.	Oct.	Nov.	Dec.
1999	Monthly rainfall (mm)	0	9	0	0	113	9	47	18	16	46	0	0
	Monthly NDVI anomalies	No data	No data	No data	No data	No data	No data	No data	No data	No data	No data	No data	No data
	Monthly temperature anomalies	0.444	0.442	−0.55	0.176	−1.46	−1.820	−0.652	−0.81	−0.33	0.396	0.639	−0.08
2000	Monthly rainfall (mm)	0	0	0	0	3	3	122	51	13	0	0	0
	Monthly NDVI anomalies	−0.017	−0.02	−0.01	−0.01	−0.02	−0.011	−0.009	−0.05	−0.05	−0.04	−0.03	−0.02
	Monthly temperature anomalies	0.676	−0.79	−1.03	0.592	−0.41	0.081	−0.104	0.376	−0.13	0.606	−0.60	0.27
2004	Monthly rainfall (mm)	0	0	1	0	1	41	20	98	21	63	0	1
	Monthly NDVI anomalies	0.039	0.033	0.025	0.024	0.023	−0.042	−0.095	−0.11	−0.06	−0.015	−0.014	−0.01
	Monthly temperature anomalies	0.056	0.280	0.934	1.075	−0.33	−0.236	0.164	0.587	−0.05	−1.774	−0.605	0.562
2005	Monthly rainfall (mm)	0	0	0	1	6	21	54	40	78	0	0	0
	Monthly NDVI anomalies	−0.015	−0.01	−0.01	−0.01	−0.01	−0.057	−0.095	−0.075	−0.03	−0.034	−0.031	−0.028
	Monthly temperature anomalies	−0.941	−1.01	−0.09	−1.48	−0.56	0.462	0.032	−0.563	0.76	−0.895	−0.359	−1.59
2014	monthly Rainfall (mm)	0	0	0	5	10	3	74	72	62	0	0	0
	Monthly NDVI anomalies	0.010	0.008	0.009	0.013	0.012	−0.054	−0.096	−0.074	−0.05	−0.038	−0.029	−0.024
	Monthly temperature anomalies	−0.992	−0.56	−0.89	−0.06	−0.09	0.900	0.750	1.070	1.25	0.511	1.577	0.056

Table 6 Areas covered by drought severity classes of SPI, SPEI, and SVI across Tharparkar during drought years of 2005 and 2014.

Drought year	Drought index (three-monthly, six-monthly)	Area covered by drought severity classes in percentage					
		Normal and wet	Abnormally dry	Moderate drought	Severe drought	Extreme drought	Exceptional drought
2005	SPI	(21,15)	(29,17)	(50,59)	(0,9)	(0,0)	(0,0)
	SPEI	(13,25)	(31,28)	(56,47)	(0,0)	(0,0)	(0,0)
	SVI	(9,5)	(11,8)	(27,26)	(31,32)	(16,21)	(6,8)
2014	SPI	(74,9)	(26,39)	(0,52)	(0,0)	(0,0)	(0,0)
	SPEI	(5,0)	(3,0)	(42,25)	(50,75)	(0,0)	(0,0)
	SVI	(6,6)	(10,7)	(21,21)	(30,33)	(26,25)	(7,8)

affected by severe drought. Diplo on the whole was affected by abnormal dry conditions. Agricultural drought severity extended further in spatial extent as exhibited by meteorological drought. During 2005, meteorological and agricultural drought severity maps depicted central, southern, northern, and northwestern parts of Tharparkar affected by moderate to severe drought while the remaining area was mostly affected by abnormally dry conditions. The 2002 drought was the worst drought year during the period under study. Tharparkar was affected by severe to exceptional drought with northwestern and southwestern parts affected by exceptional drought conditions.

5 Discussion

This study depicted average yearly temperature increase across Tharparkar from 2006 in a fluctuating manner (Fig. 3). Rise in temperature was accompanied by rise in rainfall during monsoon seasons with average rainfall ranging over 300 mm, during normal and near-normal years, to above 700 mm during monsoon seasons from 2006 to 2013 as predicted by IPCC 2007. The study characterized precipitation–vegetation interaction at monthly, three-monthly, and six-monthly temporal scales. The results depicted that vegetation was adapted to time and amount of monthly rainfall across Tharparkar with highly significant and strongly significant response from vegetation during July and August,[53–55] respectively, which was in line with findings of Lázaro et al. and Li et al. Average monthly rainfall in the monsoon season formed optimum threshold of rainfall with corresponding response from vegetation and was found consistent with previous studies.[14,53] Correlation configuration between SPI and SPEI confirmed higher loss of moisture during lower rainfall periods as presented by Vicente-Serrano.

In this study, the incorporation of SVI offered easier and meaningful insight into response of SPI and SPEI to vegetation across Tharparkar during wet and drought conditions across Tharparkar. Trend analysis of SVI with SPI and SPEI furnished vegetation response dynamics to monthly rainfall and temperature variations. It was observed that the monsoon season that received highest rainfall was not the greenest year (2011); rather the monsoon season during which monthly rainfall followed optimum pattern of rainfall was the greenest year (2010) and thus confirmed vegetation response pattern given by Li et al. for arid regions. The study presented that effect of higher positive temperature anomalies did not hamper vegetation growth response as long as monthly rainfall pattern remained at or above optimum threshold, e.g., during the wet year of 2010. The results exhibited that SPI values corresponded well with SVI under normal and wet conditions irrespective of temperature anomalies, whereas SPEI values corresponded well with SVI under normal and below normal rainfall conditions coupled with higher positive temperature anomalies.

Variation of temperature remained insignificant until rainfall remained at or higher than normal during the monsoon season across Tharparkar. The study presented that the effect of higher

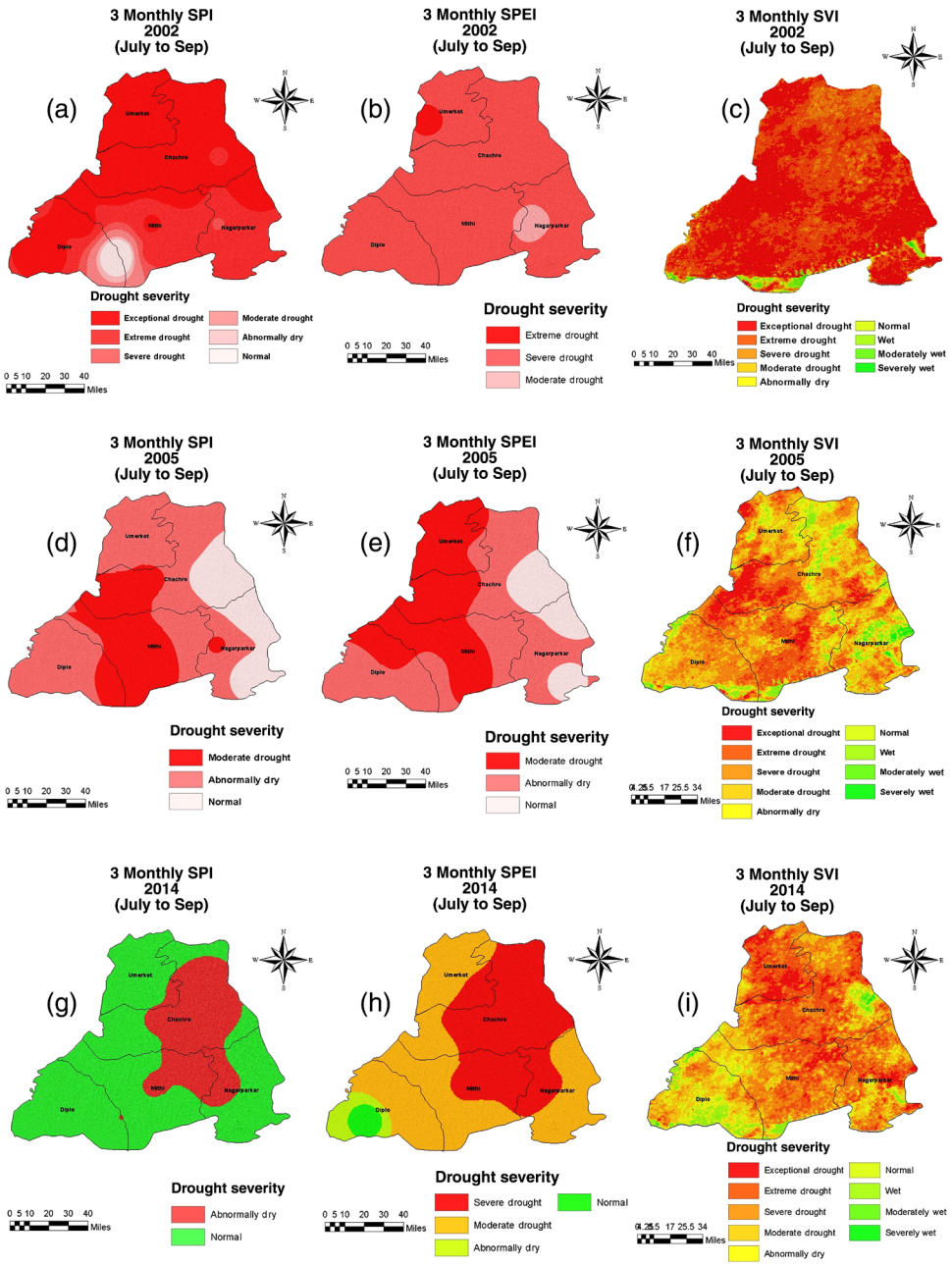

Fig. 10 Spatial variation of drought severity across Tharparkar as shown by drought indices: (a) three-monthly SPI—2002, (b) three-monthly SPEI—2002, (c) three-monthly SVI—2002, (d) three-monthly SPI—2005, (e) three-monthly SPEI—2005, (f) three-monthly SVI—2005, (g) three-monthly SPI—2014, (h) three-monthly SPEI—2014, and (i) three-monthly SVI—2014.

temperature anomalies adversely affected vegetation growth and aggravated drought severity under normal or lower than normal monthly rainfall. Lower average monthly rainfall accompanied by higher positive temperature anomalies affected cycle of vegetation growth and suppressed overall response of vegetation at agricultural scale, which was found consistent with results of a study conducted by Shaheen and Baig[16] during their research in the arid region of Thal Doab, Pakistan. The study demonstrated that negative or lower NDVI anomalies variations between consecutive monsoon seasons carried over influence of poor vegetation conditions from the previous season into the next growing season. Negative monthly NDVI anomalies before start of monsoon seasons during 2005 and 2008 depicted carryover effect of poor vegetation conditions after drought and below normal year, respectively, into the next growing

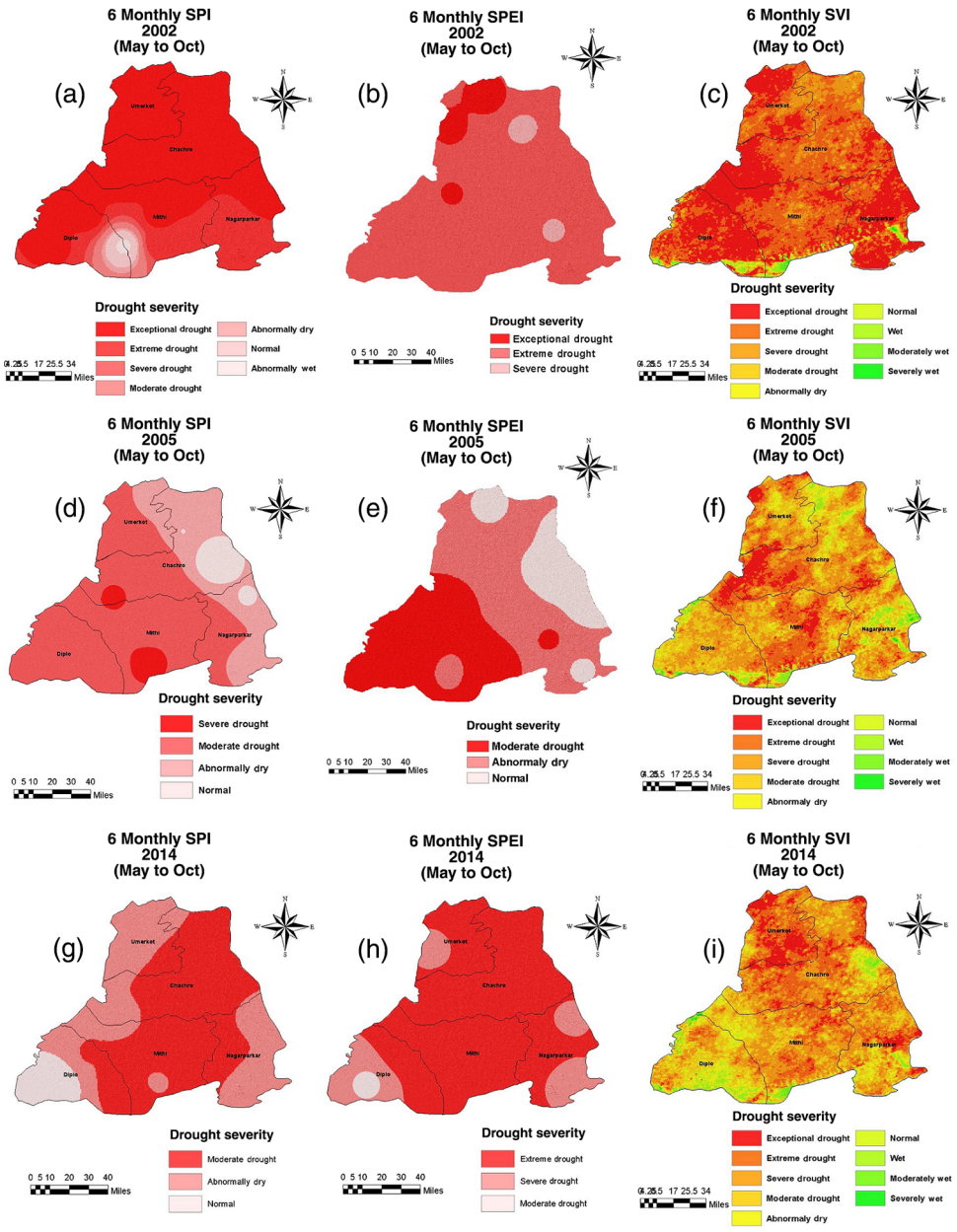

Fig. 11 Spatial variation of drought severity across Tharparkar as shown by drought indices: (a) six-monthly SPI—2002, (b) six-monthly SPEI—2002, (c) six-monthly SVI—2002, (d) six-monthly SPI—2005, (e) six-monthly SPEI—2005, (f) six-monthly SVI—2005, (g) six-monthly SPI—2014, (h) six-monthly SPEI—2014, and (i) six-monthly SVI—2014.

season thereby producing additive effect to dry or low vegetation conditions in the succeeding year.[53,56,57]

Rainfall was found to be the primary factor in initiating drought conditions across Tharparkar during drought years. Although SPI played an important role in depicting drought conditions across Tharparkar,[1,4] results of this study indicated that under drought conditions generated by lower than normal rainfall and higher temperature anomalies, role of temperature was predominant and further aggravated drought severity as predicted by Goyal,[34] during his research on future trends of drought in the neighboring arid region of Rajasthan, India. Drought years of 2005 and 2014 presented an instance when the monsoon season of 2014 received better rainfall than 2005 but faced highest positive temperature anomalies in the entire time series. SPI could not establish the effect of rise in temperature during 2014 and depicted less drought severity as compared to 2005, whereas SPEI and SVI took into account effect of temperature rise during

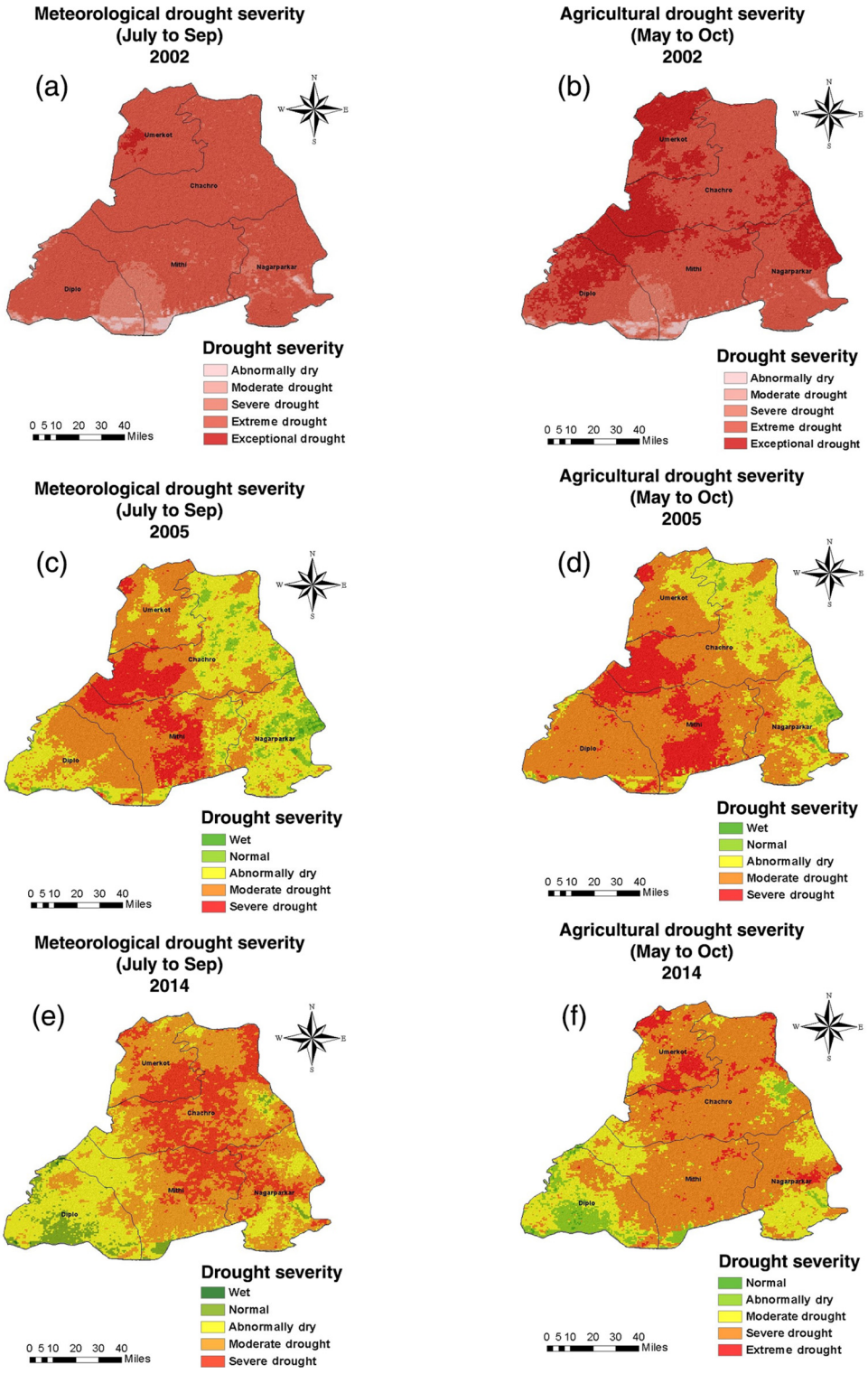

Fig. 12 Spatial variation of composite meteorological and agricultural drought severity across Tharparkar: (a) meteorological drought severity map—2002, (b) agricultural drought severity map—2002, (c) meteorological drought severity map—2005, (d) agricultural drought severity map—2005, (e) meteorological drought severity map—2014, and (f) agricultural drought severity map—2014.

2014 and depicted realistic drought conditions as against SPI. It underscored the importance of a drought index to be incorporated in analysis of drought severity, which could capture effect of increased evapotranspiration associated with rise in temperature across arid regions as suggested by previous studies under global warming scenario.[18,22,34]

Drought severity maps of SPI, SPEI, and SVI furnished isolated information about drought hazard across Tharparkar at meteorological and agricultural scales based on separate input data (Figs. 10 and 11). However, any single drought index could not establish a clear picture of spatial extent of drought severity at meteorological and agricultural drought levels. Weighted overlay analysis in GIS generated very clear spatial extents of drought severity classes across Tharparkar at both meteorological and agricultural scales (Fig. 12) as a consequence of two important steps. One was through emphasizing information of common drought severity classes captured by drought indices and another by allocation of relative weights to drought index layers, calculated through analytical hierarchy process.

The results of this study presented an effective model for drought analysis across the arid zone of Tharparkar which could be aptly implemented by utilizing freely available remote sensing data for drought hazard analysis in data scarce arid regions. Although this study confirmed effectiveness of using remote sensing data for analyzing vegetation dynamics in response to rainfall and temperature variations at coarse temporal scale of 1 month across arid region of Tharparkar, to carry out analyses for specific vegetation types detailed data such as soil moisture, vegetative growth, and crop yield would be required. The study confirmed the effectiveness and importance of a drought index that incorporated the effect of rise in temperature on drought severity across arid regions exposed to higher temperatures.

6 Conclusion

This study provided an important insight into vegetation change dynamics and drought severity across Tharparkar, which can be quite useful for relevant departments and relief agencies to respond effectively and timely in drought struck areas. The study could also be of help to the decision makers to help compensate farmers and affected people according to the drought severity in affected areas. It is recommended that local and provincial governments should take initiatives to introduce new crop varieties more resistant to evapotranspiration stress due to increased temperatures and also ensure training of local communities on rain water harvesting and soil water conservation techniques to help reduce effects of lower rainfall and higher temperatures that further aggravate drought severity. The methodology adopted for this study could be replicated on data scarce arid regions experiencing frequent droughts under higher temperatures.

References

1. T. B. McKee et al., "The relationship of drought frequency and duration to time scales," in *Proc. of the 8th Conf. on Applied Climatology*, Vol. **17**, American Meteorological Society, Boston, Massachusetts (1993).
2. S. M. Vicente-Serrano et al., "A multi-scalar drought index sensitive to global warming: the standardized precipitation and evapotranspiration index," *J. Clim.* **23**(7), 1696–1718 (2010).
3. R. Heim, "A review of twentieth-century drought indices used in the United States," *Bull. Am. Meteorol. Soc.* **83**(8), 1149–1165 (2002).
4. M. Svoboda et al., "Standardized precipitation index user guide," World Meteorological Organization Geneva, Switzerland (2012).
5. D. A. Wilhite, "Chapter 1: drought as a natural hazard: concepts and definitions," Paper 69, Drought Mitigation Center Faculty Publications, Lincoln, Nebraska (2000).
6. R. G. Allen et al., "Crop evapotranspiration—guidelines for computing crop water requirements-FAO Irrigation and drainage paper 56," *FAO Rome* **300**(9), D05109 (1998).
7. A. N. Islam et al., "Alleviation of drought stress in maize by exogenous application of gibberellic acid and cytokinin," *J. Crop Sci. Biotechnol.* **17**(1), 41–48 (2014).
8. L. M. Tallaksen and H. A. Van Lanen, "Hydrological drought: processes and estimation methods for streamflow and groundwater," Vol. **48**, Elsevier, Amsterdam, Netherlands (2004).

9. F. Perez et al., "The ITHACA early warning system for drought monitoring: first prototype test for the 2010 Sahel crisis," *Eur. J. Remote Sens.* **44**(1), 181–195 (2012).
10. G. Naumann et al., "Monitoring drought conditions and their uncertainties in Africa using TRMM data," *J. Appl. Meteorol. Climatol.* **51**(10), 1867–1874 (2012).
11. L. Du et al., "A comprehensive drought monitoring method integrating MODIS and TRMM data," *Int. J. Appl. Earth Obs. Geoinf.* **23**, 245–253 (2013).
12. J. Rhee et al., "Monitoring agricultural drought for arid and humid regions using multi-sensor remote sensing data," *Remote Sens. Environ.* **114**(12), 2875–2887 (2010).
13. A. Yaduvanshi et al., "Integrating TRMM and MODIS satellite with socio-economic vulnerability for monitoring drought risk over a tropical region of India," *Phys. Chem. Earth* **83**, 14–27 (2015).
14. R. Li et al., "Index-based assessment of agricultural drought in a semi-arid region of Inner Mongolia, China," *J. Arid Land* **6**(1), 3–15 (2014).
15. D. Dutta et al. "Assessment of agricultural drought in Rajasthan (India) using remote sensing derived vegetation condition index (VCI) and standardized precipitation index (SPI)," *Egyptian J. Remote Sens. Space Sci.* **18**(1), 53–63 (2015).
16. A. Shaheen and M. A. Baig, "Drought severity assessment in arid area of Thal Doab using remote sensing and GIS," *Int. J. Water Resour. Arid Environ.* **1**(2), 92–101 (2011).
17. M. Karabulut, "Drought analysis in Antakya-Kahramanmaraş Graben, Turkey," *J. Arid Land* **7**(6), 741–754 (2015).
18. S. M. Vicente-Serrano, "Differences in spatial patterns of drought on different time scales: an analysis of the Iberian Peninsula," *Water Resour. Man.* **20**(1), 37–60 (2006).
19. S. Khan et al., "Standard precipitation index to track drought and assess impact of rainfall on water tables in irrigation areas," *Irrig. Drain. Syst.* **22**(2), 159–177 (2008).
20. N. R. Patel et al., "Analyzing spatial patterns of meteorological drought using standardized precipitation index," *Meteorol. Appl.* **14**(4), 329–336 (2007).
21. F. Abramopoulos et al., "Improved ground hydrology calculations for global climate models (GCMs): soil water movement and evapotranspiration," *J. Clim.* **1**(9), 921–941 (1988).
22. P. Lemke et al., "The physical science basis. Contribution of working group I to the fourth assessment report of the intergovernmental panel on climate change," *Clim. Change* **2007**, 337–383 (2007).
23. L. Wang et al., "Analysis of seven-year moderate resolution imaging spectroradiometer vegetation water indices for drought and fire activity assessment over Georgia of the United States," *J. Appl. Remote Sens.* **3**(1), 033555 (2009).
24. J. Sheffield and E. F. Wood, "Projected changes in drought occurrence under future global warming from multi-model, multi-scenario, IPCC AR4 simulations," *Clim. Dyn.* **31**(1), 79–105 (2008).
25. C. S. Murthy et al., "Spatial and temporal responses of different crop-growing environments to agricultural drought: a study in Haryana state, India using NOAA AVHRR data," *Intl. J. Remote Sens.* **30**(11), 2897–2914 (2009).
26. S. M. Quiring and S. Ganesh, "Evaluating the utility of the Vegetation Condition Index (VCI) for monitoring meteorological drought in Texas," *Agric. For. Meteorol.* **150**(3), 330–339 (2010).
27. Z. Ladányi et al., "Evaluation of precipitation-vegetation interaction on a climate- sensitive landscape using vegetation indices," *J. Appl. Remote Sens.* **5**(1), 053519 (2011).
28. X. Fang et al., "Analysis of vegetation dynamics and climatic variability impacts on greenness across Canada using remotely sensed data from 2000 to 2009," *J. Appl. Remote Sens.* **8**(1), 083666 (2014).
29. X. Zhao et al., "Changing climate affects vegetation growth in the arid region of the northwestern China," *J. Arid Environ.* **75**(10), 946–952 (2011).
30. A. J. Peters et al., "Drought monitoring with NDVI-based standardized vegetation index," *Photogramm. Eng. Remote Sens.* **68**(1), 71–75 (2002).
31. S. Shahid et al., "Drought risk assessment in the western part of Bangladesh," *Nat. Hazards* **46**(3), 391–413 (2008).
32. G. M. Herani et al., "Reforming farmland and Rangeland in Tharparkar: suggested implementations for income generation," *Ind. J. Man. Social Sci.* **1**(1), 16–36 (2007).

33. A. W. Muammadi, *Why and what is Thar Development Foundation*, Chairman Thar Development Foundation care of Hyderabad X-Ray, Jail Road, Hyderabad, leaflet.
34. R. K. Goyal, "Sensitivity of evapotranspiration to global warming: a case study of arid zone of Rajasthan (India)," *Agri. Water Man.* **69**(1), 1–11 (2004).
35. A. N. Samoo, *Rain water-Harvesting (Case Studies of Rainwater Harvesting in Tharparkar)*," Tharparkar: Thardeep Rural Development Programme, Tharparkar, Sindh, Pakistan (2013).
36. R. Dodson and D. Marks, "Daily air temperature interpolated at high spatial resolution over a large mountainous region," *Clim. Res.* **8**(1), 1–20 (1997).
37. R. Sluiter, *Interpolation Methods for Climate Data: Literature Review*, Royal Netherlands Meteorological Institute (KNMI), De Bilt (2008).
38. M. Di Luzio et al., "Constructing retrospective gridded daily precipitation and temperature datasets for the conterminous United States," *J. Appl. Meteorol. Clim.* **47**(2), 475–497 (2008).
39. X. Yang et al., "Spatial interpolation of daily rainfall data for local climate impact assessment over greater Sydney region," *Adv. Meteorol.* **2015**, 1–12 (2015).
40. G. J. Huffman et al., "The TRMM multisatellite precipitation analysis (TMPA): quasi-global, multiyear, combined-sensor precipitation estimates at fine scales," *J. Hydrometeorol.* **8**(1), 38–55 (2007).
41. National Aeronautics and Space Administration, Goddard Earth Sciences Data and Information Services Center, http://disc.sci.gsfc.nasa.gov (May 2015).
42. R.S. Lunetta et al., "Land-cover change detection using multi-temporal MODIS NDVI data," *Remote Sens. Environ.* **105**(2), 142–154 (2006).
43. R. Solano et al., *MODIS Vegetation Index User's Guide (MOD13 Series)*, Vegetation Index and Phenology Lab, Tucson, Arizona (2010).
44. USGS, "MODIS products table," 2014, Land Process Distributed Active Archive Center, https://lpdaac.usgs.gov/dataset_discovery/modis/modis_products_table (May 2015).
45. National Drought Mitigation Center, "Program to calculate standardized precipitation index," http://drought.unl.edu/MonitoringTools/DownloadableSPIProgram.aspx (May 2015).
46. H. C. S. Thom "A note on the gamma distribution," *Mon. Weather Rev.* **86**(4), 117–122 (1958).
47. S. Beguería and S. M. Vicente Serrano, "SPEI calculator," 2009, https://digital.csic.es/handle/10261/10002?locale=en.
48. P. Droogers and R. G. Allen, "Estimating reference evapotranspiration under inaccurate data conditions," *Irrig. Drain. Syst.* **16**(1), 33–45 (2002).
49. T. Mavromatis, "Drought index evaluation for assessing future wheat production in Greece," *Int. J. Climatol.* **27**(7), 911–924 (2007).
50. L. Eric, US Department of Agriculture, http://droughtmonitor.unl.edu/Home.aspx (March 2015).
51. Common wealth of Australia 2016, Bureau of Meteorology,http://www.bom.gov.au/climate/austmaps/about-ndvi-maps.shtml (July 2015).
52. R. Ho-Leung, "Using analytic hierarchy process (AHP) method to prioritise human resources in substitution problem," *Int. J. Comput. Internet Man.* **9**(1), 36–45 (2001).
53. R. Lázaro et al., "Analysis of a 30-year rainfall record (1967–1997) in semi-arid SE Spain for implications on vegetation," *J. Arid Environ.* **48**(3), 373–395 (2001).
54. F. B. Turner and D. C. Randall, "Net production by shrubs and winter annuals in southern Nevada," *J. Arid Environ.* **17**(1), 23–36 (1989).
55. M. B. Bertiller et al., "Seasonal environmental variation and plant phenology in arid Patagonia (Argentina)," *J. Arid Environ.* **21**(1), 1–11 (1991).
56. W. Webb et al., "Primary productivity and water use in native forest, grassland and desert ecosystems," *Ecology* **59**(6), 1239–1247 (1978).
57. P. Haase et al., "Seed production and dispersal in the semi-arid tussock grassStipa tenacissimaL. during masting," *J. Arid Environ.* **31**(1), 55–65 (1995).

Sami Ullah Shah completed his BE degree in civil engineering in 2001. Since then he has been employed at variety of projects to include construction manager at Azad Kashmir, after

earthquake in 2005 and took active part in rehabilitation and construction works. He has also served in remote areas of Sindh, Pakistan on similar assignments. Currently, he is pursuing his MS degree in RS and GIS at Institute of Geographical Information Systems, National University of Sciences and Technology, Islamabad, Pakistan.

Javed Iqbal is an associate professor and head of department at IGIS at National University of Sciences and Technology, Islamabad, Pakistan. His PhD is in soil sciences and precision agriculture from Mississippi State University and post-doc from Purdue University, West Lafayette. He also worked with USDA-ARS facility at Starkville, Mississippi state on several precision agriculture related projects on the farmer's field in Mississippi.